

UNCLASSIFIED

A 94492

Armed Services Technical Information Agency

**Reproduced by
DOCUMENT SERVICE CENTER
KNOTT BUILDING, DAYTON, 2, OHIO**

This document is the property of the United States Government. It is furnished for the duration of the contract and shall be returned when no longer required, or upon recall by ASTIA to the following address: Armed Services Technical Information Agency, Document Service Center, Knott Building, Dayton 2, Ohio.

**NOTICE: WHEN GOVERNMENT OR OTHER DRAWINGS, SPECIFICATIONS OR OTHER DATA
ARE USED FOR ANY PURPOSE OTHER THAN IN CONNECTION WITH A DEFINITELY RELATED
GOVERNMENT PROCUREMENT OPERATION, THE U. S. GOVERNMENT THEREBY INCURS
NO RESPONSIBILITY, NOR ANY OBLIGATION WHATSOEVER; AND THE FACT THAT THE
GOVERNMENT MAY HAVE FORMULATED, FURNISHED, OR IN ANY WAY SUPPLIED THE
SAID DRAWINGS, SPECIFICATIONS, OR OTHER DATA IS NOT TO BE REGARDED BY
IMPLICATION OR OTHERWISE AS IN ANY MANNER LICENSING THE HOLDER OR ANY OTHER
PERSON OR CORPORATION, OR CONVEYING ANY RIGHTS OR PERMISSION TO MANUFACTURE,
USE OR SELL ANY PATENTED INVENTION THAT MAY IN ANY WAY BE RELATED THERETO.**

UNCLASSIFIED

AD NO. 24492

ASTM FILE COPY



FC

THE MEASUREMENT OF THE ABSOLUTE
ENERGY OF LOW ANGLE DISLOCATION
BOUNDARIES IN ZINC

FOURTEENTH TECHNICAL REPORT

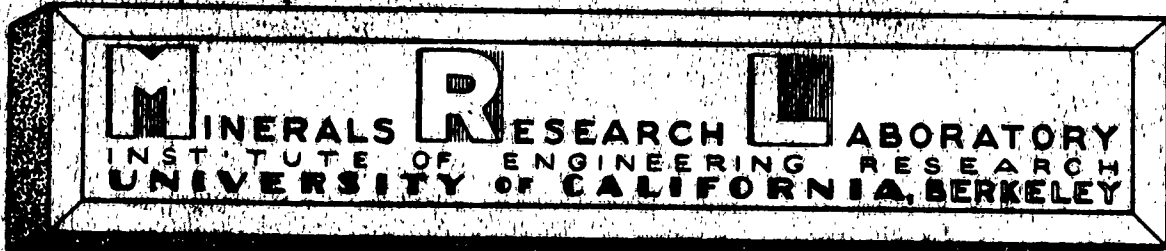
BY

R. B. SHAW
T. L. JOHNSTON
R. J. STOKES
J. WASHBURN
E. R. PARKER

MAY, 1956

SERIES NO. 27 ISSUE NO. 14

CONTRACT N7-ONR-29516 NR031-255



THE MEASUREMENT OF THE ABSOLUTE ENERGY OF LOW
ANGLE DISLOCATION BOUNDARIES IN ZINC

Fourteenth Technical Report

By

Robert B. Shaw
T. L. Johnston
R. J. Stokes
Jack Washburn
E. R. Parker

Office of Naval Research Project

N7-onr-29516 NR 031-255

May, 1956

University of California
Berkeley, California

Issue No. 114
Series No. 27

INTRODUCTION

The first real impetus to the study of dislocation boundaries in crystals came as a result of a proposal by Burgers⁽¹⁾ and Bragg⁽²⁾ that edge dislocations stacked in a plane perpendicular to the slip plane should be stable. The discovery of subgrain structures and the polygonization process revealed that low angle boundaries were frequently present in crystals grown from the melt and that they could be introduced into crystals through plastic deformation and annealing⁽³⁾⁽⁴⁾. An approach to the problem of grain boundary energies was suggested by C. S. Smith⁽⁵⁾ who considered the equilibration of the interfacial tensions of boundaries in tri-grain junctions as a means of measuring relative interfacial energies. By growing tricrystals containing one boundary of a predetermined disorientation, Dunn, and Lionetti⁽⁶⁾, and Dunn, Daniels and Bolton⁽⁷⁾, succeeded in determining relative boundary energies as a function of degree of disorientation for (100) and (110) boundaries in silicon iron. These data were found to agree quite well with an equation for low angle boundary energy derived from a dislocation model by Shockley and Read⁽⁸⁾⁽⁹⁾. Other evidence further substantiated the dislocation model for low angle boundaries. Parker and Washburn⁽¹⁰⁾⁽¹¹⁾ discovered that low angle boundaries in zinc single crystals would move upon the application of a shear stress. Lastly, the proof that low angle tilt boundaries are made up of rows of discrete elements was supplied by Vogel, Pfann, Corey and Thomas⁽¹²⁾ who produced a photomicrograph of a low angle boundary showing a straight row of equally spaced etch-pits in a germanium crystal. The spacing of these pits was accounted for by the angular tilt of the boundary, assuming that the position of each pit indicated the location of an edge dislocation.

There is little doubt that Parker-Washburn low angle boundaries are made up of edge dislocations. This being the case, the Shockley-Read formula

$$E = E_0 \theta \ln \left[\theta_m e / \theta \right] \dots \dots \dots \quad (1)$$

should be applicable to such boundaries, where E is the specific interfacial energy, E_0 and θ_m are constants, and θ the angle of tilt. The constant E_0 may be calculated from the elastic properties of the material. For an isotropic elastic solid

$$E_0 = \frac{G |b|}{4\pi(1-\nu)}$$

where G is the shear modulus, b is the Burgers vector, and ν is Poisson's ratio. Several anisotropic cases have been treated by A. J. E. Foreman⁽¹³⁾.

The theoretical knowledge of θ_m is somewhat uncertain. This difficulty is a reflection of the inadequacy of the dislocation model to define the core. The core energy of a dislocation is not calculable, neither is the interaction of the stress field of neighboring dislocations with the core. An approximate value of θ_m may be obtained by fitting the reduced form of equation (1) to relative energy measurements. These measurements have been carried out on silicon iron by Dunn et al⁽⁶⁾⁽⁷⁾, on tin and lead by Aust and Chalmers⁽¹⁴⁾, and on silver by Greenough and King⁽¹⁵⁾. The approximate values of θ_m obtained are as follows:

Silicon Iron (100)	30°
Silicon Iron (110)	27°
Lead	25°
Tin	12°
Silver	25°

It should be pointed out that these values of θ_m are subject to an uncertainty of several degrees as a result of scatter in the data. In addition, θ_m is probably a function of θ . Consequently, the θ_m which produces a good fit at high angles need not be the same as the θ_m which applies at low angles.

Adding a constant core energy per dislocation to the Shockley-Read formula merely changes the value of the constant θ_m . Hence the formula has, in a sense, a built-in constant core energy per dislocation. In spite of a lack of knowledge of the value of θ_m , the Shockley-Read formula should provide a reasonably correct functional dependence of energy on θ for small angles.

In studies on the stress induced motion of low angle boundaries, it was discovered⁽¹⁶⁾⁽¹⁷⁾ that at low temperatures, motion was accompanied by a decrease in boundary angle, whereas, at temperatures above 300°C, the boundary angle remained constant. At low temperatures, shear stresses of the order of the yield stress were necessary for motion, while at temperatures above 300°C there was no lower limit to the stress for boundary motion. The edge dislocations in these boundaries move parallel to slip planes in the absence of dislocation climb. Hence, a one to one correspondence exists between the crystal geometry and the position of a boundary as shown in Fig. 1. These facts suggested that absolute energy measurements were possible, provided a system could be devised in which the total free energy as a function of boundary position passed through a minimum, and provided some measurable external force contributed to the energy. Such a system is shown schematically in Fig. 2. The figure depicts a single crystal in the form of a thin triangular plate containing a small angle boundary at **FE** introducing a tilt θ . The specimen is supported at the tip **A** so that the

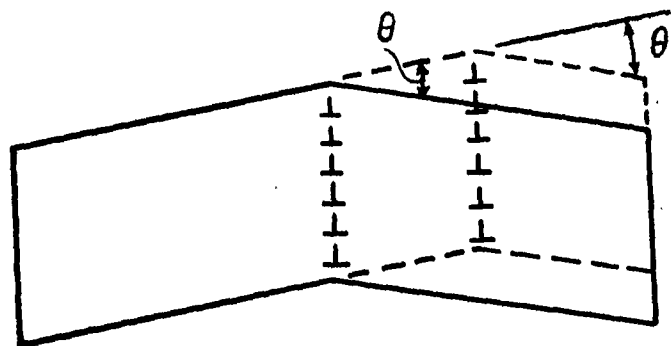


FIG. 1 THE CHANGE IN GEOMETRY CORRESPONDING TO THE DISPLACEMENT OF AN EDGE BOUNDARY.

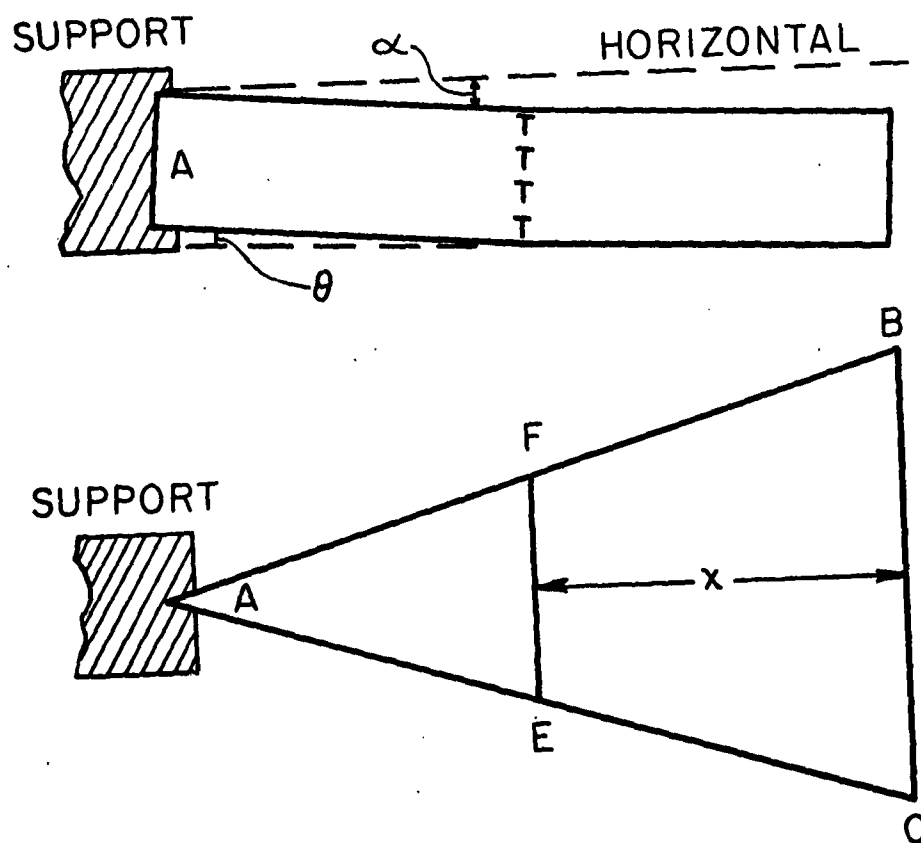


FIG. 2 THE ELEVATION (a) AND PLAN (b) OF A THIN TRIANGULAR CRYSTAL WITH A LOW ANGLE BOUNDARY AT FE.

plane AFE makes an angle α with the horizontal. It may be seen in an elementary way, that for values of $\alpha \approx 0$, the free energy of the boundary decreases with decreasing distance from A due to the reduction in cross-sectional area; however, the potential energy of the crystal increases as the distance between A and the boundary decreases.

The success of an experiment of this kind depends on the ability of a low angle boundary to move under the action of forces arising from the change in surface-free energy alone. This was confirmed by the microscopic observation of a low angle boundary in a small tapered zinc crystal which was heated to within a few degrees of the melting point. This boundary moved at a rate of several microns per hour in the absence of external forces.

Analysis of the Single Boundary Experiment

The essential geometrical features of the specimen shown in Fig. 2 are represented analytically in Fig. 3. The simple case in which $\alpha = 0$ will be treated here. The more complex solution for the general case, in which α is variable, is presented after the derivation for the simple case. In Fig. 3, A represents the point of support and C the base of the triangular crystal. The boundary divides the crystal into two parts, designated I and II in the figure. The problem can be treated as though the mass of each part were concentrated at its respective center of gravity. Point E represents the position of the boundary, a distance x from the base; point P represents the center of gravity of part II of the crystal. The interfacial free energy of the boundary is given by:

$$F_s = 2 t (L - x) \tan \phi \gamma$$

where γ is the specific interfacial free energy of the boundary. The

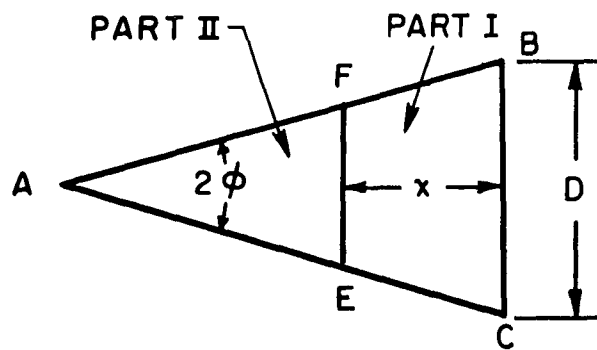
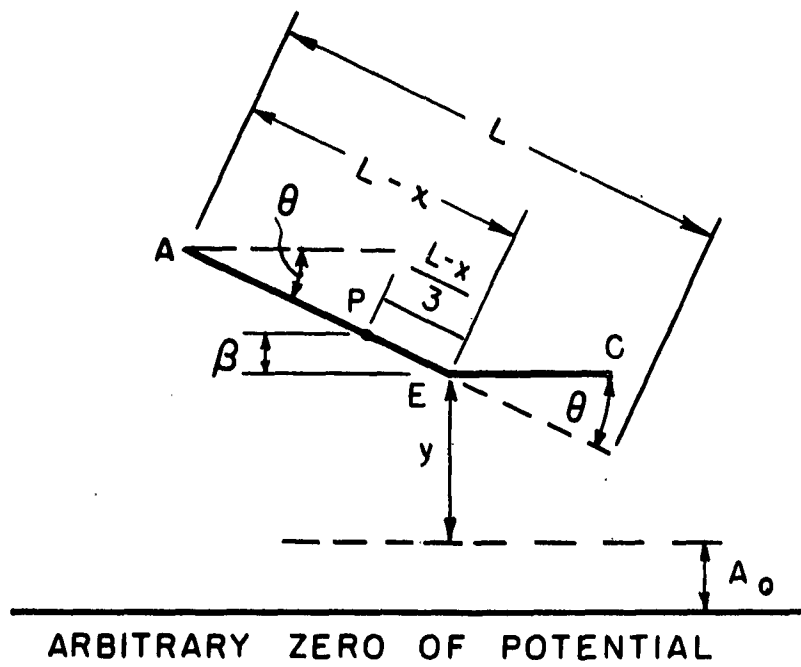


FIG. 3 ANALYTICAL REPRESENTATION OF A TRIANGULAR SPECIMEN FOR THE PURPOSE OF CALCULATION OF THE FREE ENERGY FOR THE SPECIAL CASE $\alpha = \theta$

potential energy of part I above an arbitrary zero of potential is:

$$F_I = \delta V_I g (A_0 + y)$$

where δ is the density of the crystal, V_I the volume of part I, and g the acceleration of gravity. From the geometry

$$V_I = tx (D - x \tan \theta)$$

$$y = x \sin \theta$$

Substitution reveals that

$$F_I = \delta g t x (D - x \tan \theta) (A_0 + x \sin \theta)$$

The potential energy of part II above the same zero of potential is given as

$$F_{II} = \delta g V_{II} (A_0 + y + \beta)$$

where V_{II} is the volume of part II. From the geometry

$$V_{II} = t (L - x)^2 \tan \theta$$

$$y = x \sin \theta$$

$$\beta = 1/3 (L - x) \sin \theta$$

therefore

$$F_{II} = \delta g t \tan \theta (L - x)^2 [A_0 + x \sin \theta + 1/3 (L - x) \sin \theta]$$

The total free energy F_T is the sum of the components

$$F_T = F_s + F_I + F_{II}$$

or

$$F_T = 2t (L - x) \tan \theta \gamma + \delta g t x (D - x \tan \theta) (A_0 + x \sin \theta) + \delta g t \tan \theta (L - x)^2 [A_0 + x \sin \theta + 1/3 (L - x) \sin \theta]$$

Since the zero of potential was arbitrary, one may set

$$A_0 = 0$$

Then

$$F_T = 2t (L - x) \tan \theta \gamma + \delta g t x^2 \sin \theta (D - x \tan \theta) + \delta g t \tan \theta (L - x)^2 [x \sin \theta + 1/3 (L - x) \sin \theta]$$

Setting $\frac{dF_T}{dx} = 0$ and solving for γ one obtains

$$\gamma = \delta g \sin \theta x_0 \left[L - \frac{x_0}{2} \right] \dots \dots \dots \quad (2)$$

since

$$L = \frac{D}{2 \tan \phi}$$

where x_0 is the equilibrium value of x . It can be shown that the free energy has a minimum and not a maximum by the sign of the second derivative, and that this minimum exists within the bounds of the crystal.

The solution to the general case where α is variable, is as follows:

$$\begin{aligned} \gamma = & \frac{1}{2} \frac{\delta g D x_0}{\tan \phi} \left\{ \sin \alpha - 2 \sin (\alpha - \theta) \right\} \\ & - \frac{1}{2} \delta g x_0^2 \left\{ \sin \alpha - 3 \sin (\alpha - \theta) \right\} \\ & + \frac{1}{2} \delta g D \sin (\alpha - \theta) \left\{ 2x_0 \left[\frac{3D - 4x_0 \tan \phi}{6D - 6x_0 \tan \phi} \right] - \frac{Dx_0^2 \tan \phi}{6(D - x_0 \tan \phi)^2} \right\} \\ & - \frac{1}{2} \delta g \sin (\alpha - \theta) \left\{ 3x_0^2 \left[\frac{3D - 4x_0 \tan \phi}{6D - 6x_0 \tan \phi} \right] - \frac{Dx_0^3 \tan \phi}{6(D - x_0 \tan \phi)^2} \right\} \end{aligned}$$

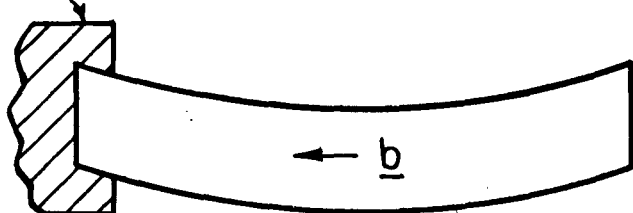
When $\alpha = \theta$, this expression for γ reduces to the simpler case just derived.

If γ in the above expression is expanded into a Taylor's Series in α , one finds that the partial derivatives $\frac{\partial \gamma}{\partial \alpha}$, $\frac{\partial^2 \gamma}{\partial \alpha^2}$, etc., are identically zero in the neighborhood of $\alpha = \theta$, providing the additional assumption is made that $\cos \theta = \cos \alpha = 1$ for small angles. Since γ is insensitive to small changes in α , the latter angle may be $\pm 5^\circ$ from the ideal value $\alpha = \theta$ and the simpler equation (2) may still be used.

Analysis of the Bent Crystal Experiment

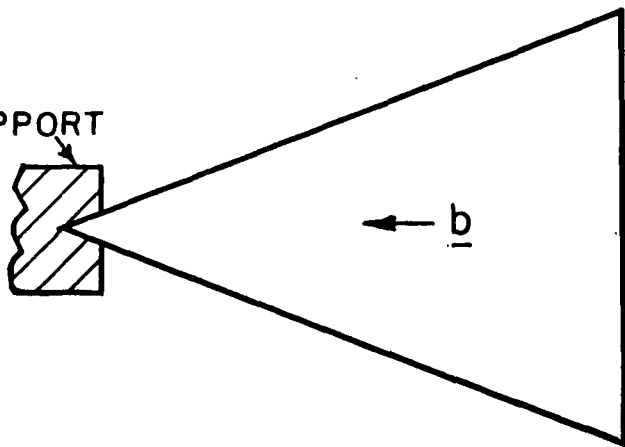
A variation of the type of specimen just discussed is shown in Fig. 4. It consists of a triangular crystal bent to a uniform curvature and supported

SUPPORT



(a)

SUPPORT



(b)

FIG. 4 TRIANGULAR CRYSTAL BENT ABOUT AN AXIS NORMAL TO
THE PLANE OF THE PAPER.
(a) ELEVATION VIEW, (b) PLAN VIEW.

by its tip in the manner shown. This type of specimen has some advantages, as the following discussion will show.

Consider first a thin rectangular shaped single crystal plate which has been bent plastically about an axis normal to the slip vector. The slip planes become circular cylinders with a radius R . This bending is accommodated by a uniform "random" distribution of positive edge dislocations whose density is $1/Rb$ per unit area normal to the dislocation lines of Burgers Vector b . If this crystal were heated to a high temperature for a sufficiently long period of time, the dislocations would redistribute themselves into a stable array of nearly parallel, low angle boundaries. The following argument attempts to show that the boundary angles in this stable array would tend to be alternately greater and smaller than the average $\bar{\theta}$. Before annealing, the dislocation density is constant over volumes of the order of \bar{S}^3 , where \bar{S} is the average final boundary spacing. Neglecting end effects, the boundary dislocations cannot escape except by climb. Considering the strong local interaction between dislocations, it is reasonable to assume that the probability of a given dislocation moving a distance greater than \bar{S} without being absorbed into a low angle boundary is very small. Thus, if for some reason one boundary angle has grown larger than the average, it has done so at the expense of its immediate neighbors who are competing for the same dislocations. This tends to produce an array of alternate high and low boundary angles. Let us call this the "normal" distribution.

If a homogeneous shear stress is applied to the rectangular crystal in the slip direction at high temperature, the smaller angle boundaries in the array will move at a faster rate than the larger ones⁽¹⁶⁾ and will eventually overtake and become absorbed in the slower moving boundaries.

Thus, a new array will be formed as a result of application of stress, which will be characterized by a larger $\bar{\theta}$ and \bar{S} than normal. Let us call this the "perturbed" distribution.

If now a specimen in the shape of a triangular plate, mounted by the tip as shown in Fig. 4, is uniformly bent and heated for a long period of time at a high temperature, it will form an array of low angle boundaries as in the above case. Corresponding to the average boundary angle there is an equilibrium position for which the force $-\frac{dF_a}{dx}$ is cancelled by the force $-\delta(\frac{F_I + F_{II}}{dx})$. Near this equilibrium position there is a tendency for the boundaries to assume the "normal" distribution. Away from this position, the above forces are active and bring about the "perturbed" state. Hence, by locating the region where the "normal" state exists, and measuring the average boundary angle in the "normal" state, one may apply the equation:

$$\gamma_N = \delta g \sin \bar{\theta}_N x_N \left[L - \frac{x_N}{2} \right]$$

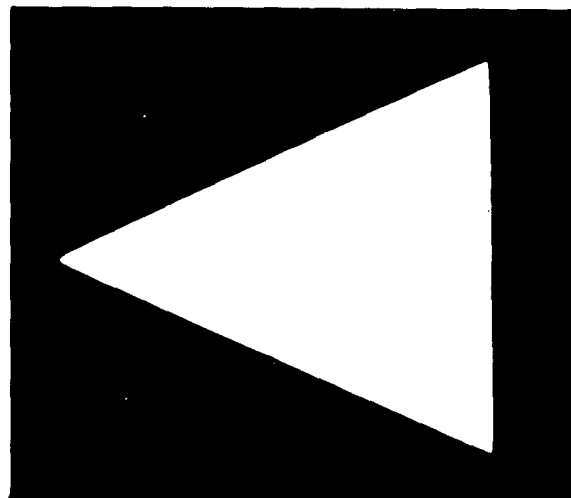
where γ_N is the specific free interfacial energy corresponding to the normal state boundary angle $\bar{\theta}_N$, and x_N is the distance of the normal region from the base of the specimen. The justification for the application of this single boundary equation to the multiple boundary case is that after a sufficiently long isothermal treatment the boundaries in the "normal" state will no longer interact, and second, that the expression for energy as a function of α does not change with α in the region where $\cos \alpha \approx 1$.

Experimental Procedure

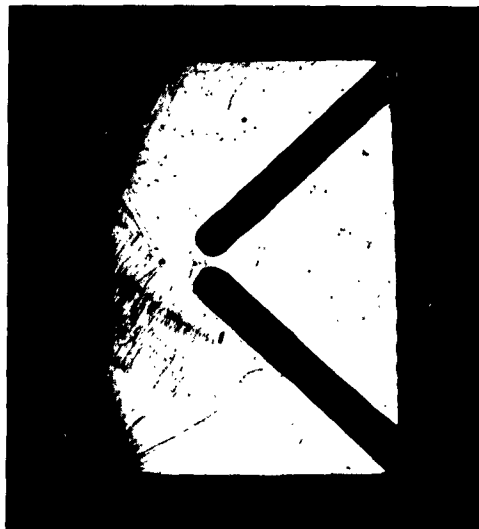
Several zinc single crystal spheres were grown from the melt as a preliminary step in the preparation of the triangular specimens. Two

types of specimens were used in this investigation, as shown in Fig. 5 (a) and (b). The first, a simple triangular plate, was employed in both the single and multiple boundary experiments. However, this type of specimen proved inconvenient in that it had to be cemented to a support. The second type of specimen did not require cement because the triangular portion was connected to the mother crystal.

The first type of specimen was prepared by acid-sawing and cleaving. The first three acid cuts produced an isosceles triangular prism in which the c-axis was oriented parallel to the elements of the prism and the slip direction was perpendicular to the base. Figure 6 shows a photograph of the stainless steel alignment jig which was designed to remove the triangular prism accurately from a one-inch diameter spherical crystal by acid-sawing. This prism was next acid-sawed into triangular plates one eighth of an inch thick. Each plate was chemically polished in concentrated nitric acid and washed in distilled water. Finally a thin wafer was cleaved from each of the two outer faces, leaving a thin triangular plate with polished sides and flat parallel faces. Figure 7 shows an arrangement that was devised for the purpose of cleaving thin plates without deforming them. The specimen at "A" was placed with one face against a flat cleavage face "B" of a large zinc crystal, and a drop of ethyl alcohol inserted at "C" between the two faces. A thin layer of silicone grease was spread on the top face at "D" and covered with a piece of cardboard at "E". The whole assembly was cooled in liquid nitrogen at which temperature the ethyl alcohol and the silicone grease were frozen. The silicone grease and the cardboard provided reinforcement for the thin wafer of zinc to be cleaved away. Without this precaution it was found that the thin piece would break off part way across the plane of cleavage. The frozen alcohol cemented the



(a)



(b)

FIG. 5 TYPES OF SPECIMENS USED

(a) SIMPLE TRIANGULAR 4X.

(b) SMALLER TYPE CONTAINING A
LOW ANGLE BOUNDARY. 10X.

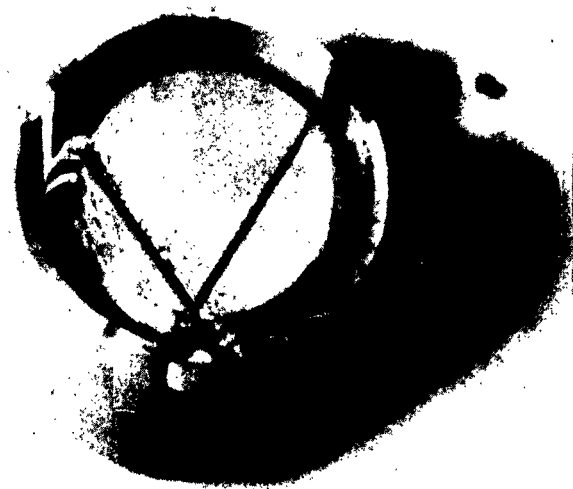


FIG. 6 ALIGNMENT JIG FOR CUTTING SINGLE CRYSTAL TRIANGULAR PRISMS.

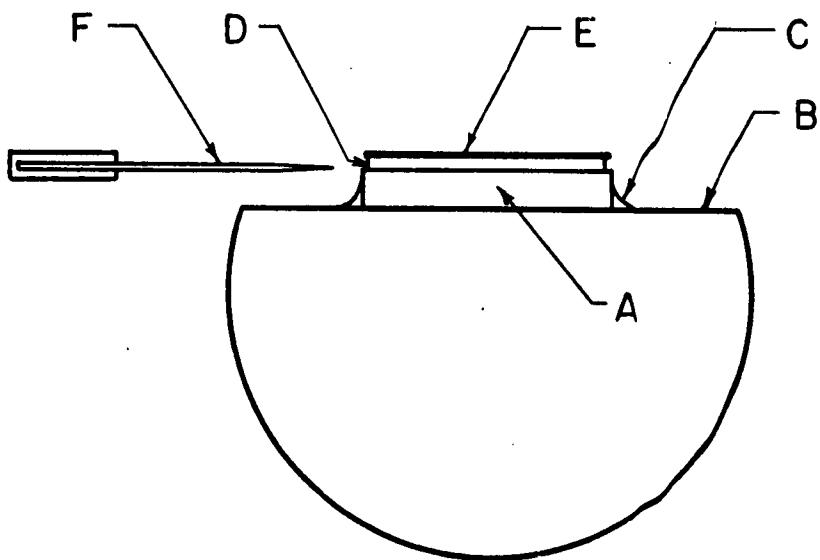


FIG. 7 ARRANGEMENT FOR CLEAVING
THIN ZINC CRYSTALS

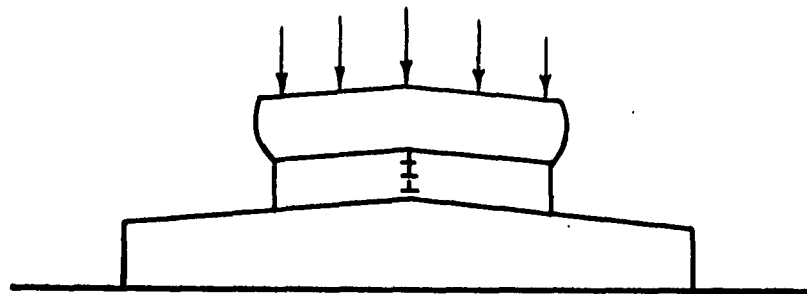
- A. ZINC SINGLE CRYSTAL SPECIMEN
- B. LARGE ZINC SINGLE CRYSTAL
- C. ETHYL ALCOHOL
- D. SILICONE GREASE
- E. CARDBOARD
- F. RAZOR BLADE

specimen rigidly to the larger crystal, and thus prevented any deformation of the specimen. The alcohol was washed away later leaving an uncontaminated surface. Finally, a low angle boundary was introduced by pressing the crystal against a die as shown in Fig. 8 (a).

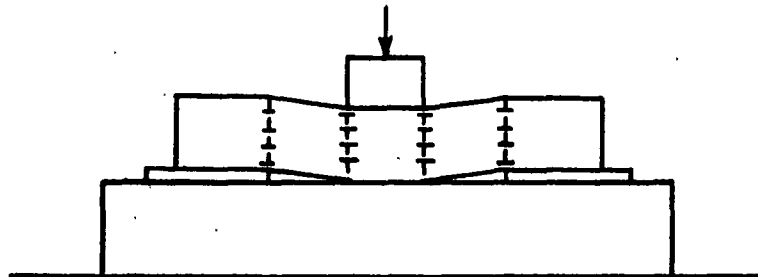
The second type of specimen (shown in Fig. 5(b)) was prepared as follows. A one-quarter inch square by one inch long prism was acid-sawed from a spherical crystal; the c-axis was oriented normal to one set of side faces and the slip direction was parallel to the edges of the prism. Four widely spaced boundaries were introduced by kinking the crystal as in Fig. 8 (b), and annealing at 400°C. The rectangular specimen was mounted in a tilting jig which was placed on the acid-saw as shown in the photograph in Fig. 9. This provided a means of making the two oblique partial cuts. Individual specimens were sectioned, each having a single low angle boundary included in the triangular portion, and the preparation was completed by cleavage off the outer surfaces.

The specimens used in the bent crystal experiments were simple triangular plates whose preparation has been described. These crystals were bent plastically to a large radius of curvature by pressing them against the surface of a smooth glass tube with a thick rubber pad. The radius of the tube used was 4.23 centimeters. Subsequently, the specimens were supported at the tip in a horizontal position, with the concave surface uppermost, and then heated for 168 hours at 412°C. After removal from the furnace, a survey was made of the interboundary spacings, the boundary positions, and the boundary angles.

For the purpose of heating the specimens at 412°C the tube furnace shown as "A", in Fig. 10, was employed. The furnace was mounted on sliding ways "B" so that it could be shifted to the alternate position at "C".



(a)



(b)

FIG. 8 METHODS OF INTRODUCING LOW ANGLE BOUNDARIES.

**(a) PRESSING AGAINST A GLASS DIE WITH
A RUBBER PAD ,**

(b) DOUBLE KINK METHOD .



TOP VIEW

FIG. 9 TILTING JIG IN POSITION ON ACID-SAW.
ON THE RIGHT AND LEFT ARE CONTAINERS
FOR NITRIC ACID. THE SPECIMEN RESTS
LIGHTLY AGAINST THE WIRE WHICH
OSCILLATES PARALLEL TO ITS AXIS
CARRYING ACID TO THE SPECIMEN.

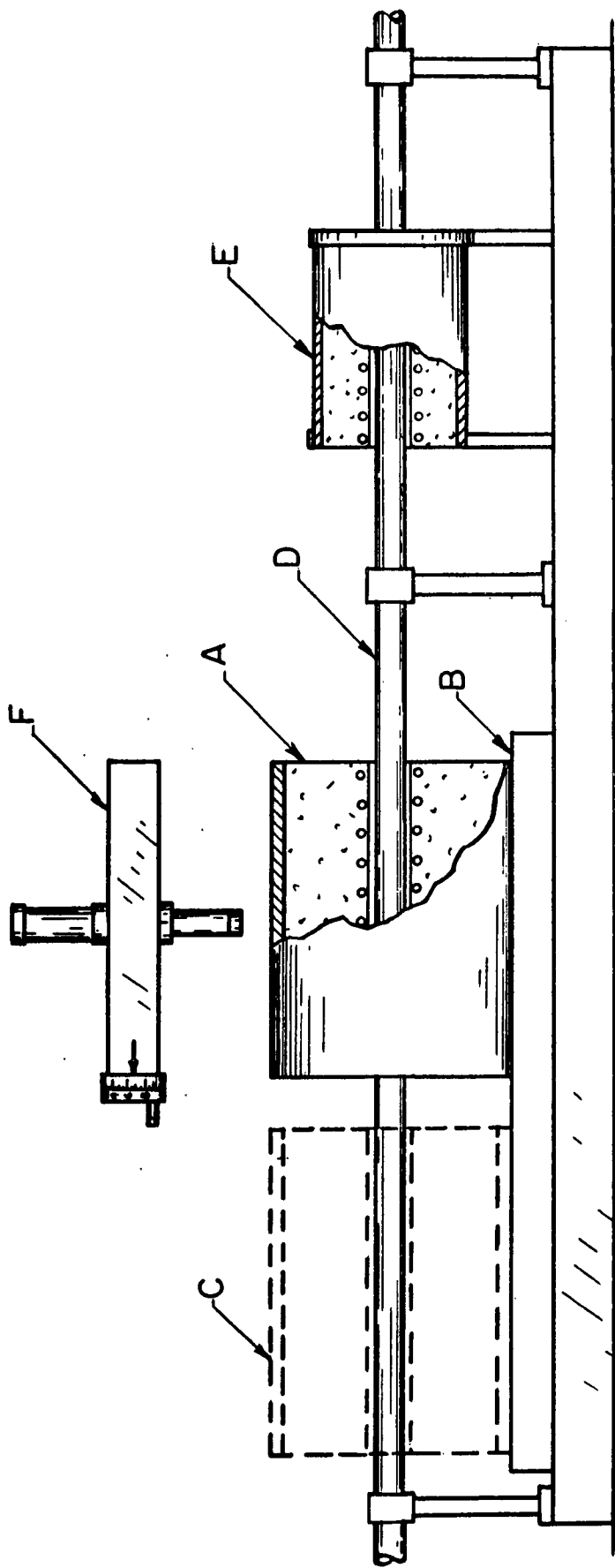


FIG. 10 FURNACE ASSEMBLY. A-TUBE FURNACE, B-SLIDING WAYS, C-ALTERNATE FURNACE POSITION, D-PYREX GLASS TUBE, E-SMALL FURNACE, F-MEASURING MICROSCOPE.

After the specimens had been heated for a period of time the furnace was permitted to cool and then shifted to the alternate position. The measurement of the boundary positions could then be made with the aid of a traveling microscope at "F", through a flat window in the long pyrex tube "D". Helium gas was directed through a silica gel-magnesium perchlorate drying tower into the pyrex tube, and then over calcium chips heated to 475°C by the small furnace at "E". The specimens were placed in a zinc boat which supported them in a way that allowed free overhang of the triangular plates. The boat was placed in a sheet molybdenum box whose sliding top could be pulled to one side by a magnet without opening the system.

Results of the Single Boundary Experiments

The dimensions of the nine specimens used in this investigation are presented in Table I. The uncertainty in the measurement of the boundary angle θ was less than $\pm 0.01^{\circ}$. The uncertainty in the length measurements was ± 0.0002 centimeter, and the uncertainty in the apex angle 2θ was $\pm 0.1^{\circ}$. All measurements were made at room temperature.

Table II shows the boundary positions tabulated against the number of hours of isothermal treatment at 412°C . Specimens 1, 2, and 3 were the simple triangular type shown in Fig. 5 (a), while specimens 4 through 9 were the smaller type shown in Fig. 5 (b). They did not all contain single boundaries at the start, as indicated in Table II. Specimens 1, 2, 3, 5, and 9 had single boundaries from the start, while specimens 4, 6, 7, and 8 had a set of closely spaced parallel boundaries. Those in 4 and 6 eventually coalesced into single boundaries but those in 7 and 8 did not.

Out of the nine specimens, only those numbered 1, 2, 4, and 5 produced significant results. The boundaries in specimens 3 and 9 did not move far enough to establish their direction of motion. Specimens 7 and 8 still contained double boundaries after 321 hours; specimen 6 still

contained a very low angle skew boundary which intersected the main boundary.

From a knowledge of the position and direction of motion of a boundary it was possible to calculate either an upper or a lower limit of interfacial free energy by using the previously derived equation (2). A moving boundary is one which is moving toward but has not reached equilibrium. If a boundary moves from its instantaneous position x_i , its energy is either less than or greater than the value $\gamma(x_i)$ depending on whether it is moving away from or towards the tip of the specimen respectively.

Using the data tabulated in Table I and Table II, the free energy limits were calculated for specimens numbered 1, 2, 4, and 5. The results are presented in Table III.

TABLE I
Specimen Dimensions at 25°C

Spec. No.	θ Deg.	D Cm.	2ϕ Deg.	t Cm.
1	1.18	1.1473	63.3	0.1404
2	1.61	1.3979	49.3	0.1751
3	1.00	1.3365	49.8	0.2582
4	0.59	0.4900	93.7	0.0989
5	0.68	0.4581	85.0	0.1152
6	2.19	0.4837	73.0	0.1404
7	1.59	0.4634	73.0	0.1133
8	0.91	0.4890	43.5	0.1643
9	0.73	0.4745	43.7	0.1497

TABLE II

Position of the Boundaries in Centimeters from the Base Measured at 25°C after Heating at 412°C

Spec. No.	Initial Position	After 45 Hrs.	After 135 Hrs.	After 321 Hrs.	Final Position
1*	0.4366				0.4410
2	1.0360			1.0340	1.0340
3	0.2867			0.2867	0.2867
4**	0.0412 0.0555 0.0785	0.0776 0.0888	0.0865	0.1255	0.1255
5	0.1299	0.1335	0.1335	0.1335	0.1335
6**	0.1537 0.1620 0.1673	0.1651 0.1190	0.1645 0.1182	0.1634 0.1191	0.1634 0.1191
7**	0.1199 0.1309 0.1147	0.1190 0.1452	0.1182 0.1457	0.1191 0.1392	0.1191 0.1392
8**	0.1372 0.1473	0.1352 0.1449	0.1349 0.1485	0.1354 0.1477	0.1354 0.1477
9	0.1535	0.1535	0.1532	0.1531	0.1531

* Specimen was heated for 670 hours at 412°C.

** Specimen initially had several boundaries.

TABLE III

The Limits of γ Ergs/Cm²

Spec. No.	θ Deg.	Limit of Energy Ergs/Cm ²
1	1.18	Greater than 44
2	1.61	Less than 288
4	0.59	Greater than 15
5	0.68	Greater than 19

Results of the Bent Crystal Experiment

The dimensions of the specimens are presented in Table IV. These were pressed against a cylindrical glass die of radius 4.23 cm. but due to elastic spring back, the specimen radii were approximately 5 percent greater than the die radius. The final disposition of the low angle boundaries after isothermal annealing is illustrated in the photomicrograph of specimen 2-B in Fig. 11. In Fig. 12 (a) and (b) the mean of the two interboundary spacings, \bar{S} , found on either side of a given boundary has been plotted as a function of the order in which the boundaries occur from the base. Each plot is characterized by a region of closely spaced boundaries which are identified with the region of the "normal" distribution. These graphical plots do not allow the two limits of the "normal" region to be determined. In each case the more clearly defined transition from the "normal" to the "perturbed" region is indicated by the short arrow. In Fig. 12 (a) the boundaries to the right of the arrow move toward the base so that this value is associated with an upper energy limit, whereas in Fig. 12 (b) the converse applies. Table V presents the energy limits calculated from equation (2) for the maximum and minimum boundary angles measured in the "normal" region.

TABLE IV
Dimensions of Specimens Used in the Bent
Crystal Experiment

Spec. No.	D Cm.	2ϕ Deg.	Die Radius Cm.	t Cm.
1-B	1.410	48.9	4.23	0.179
2-B	0.8577	57.2	4.23	0.133

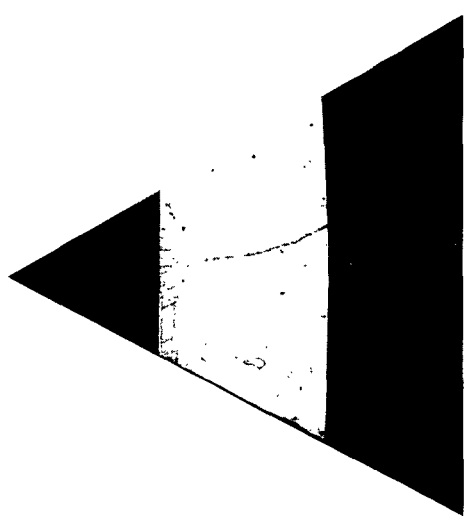
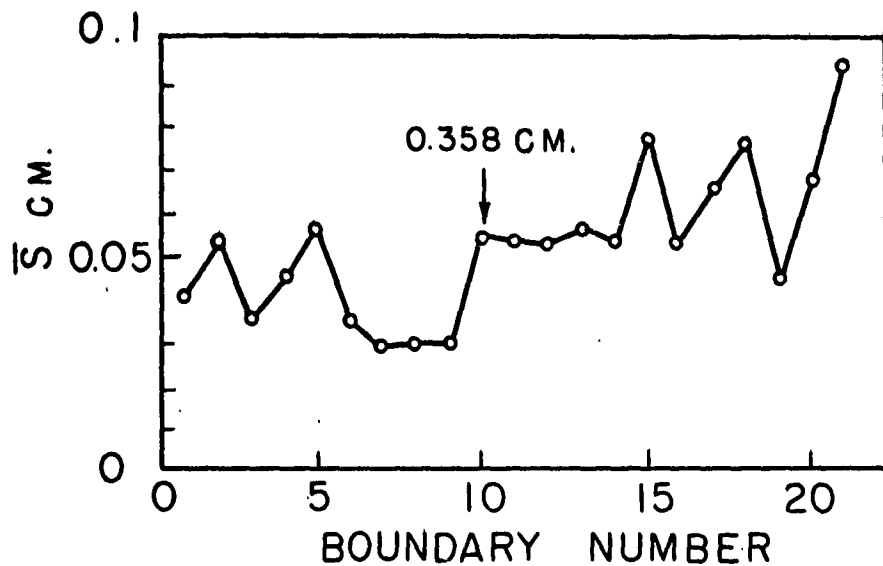
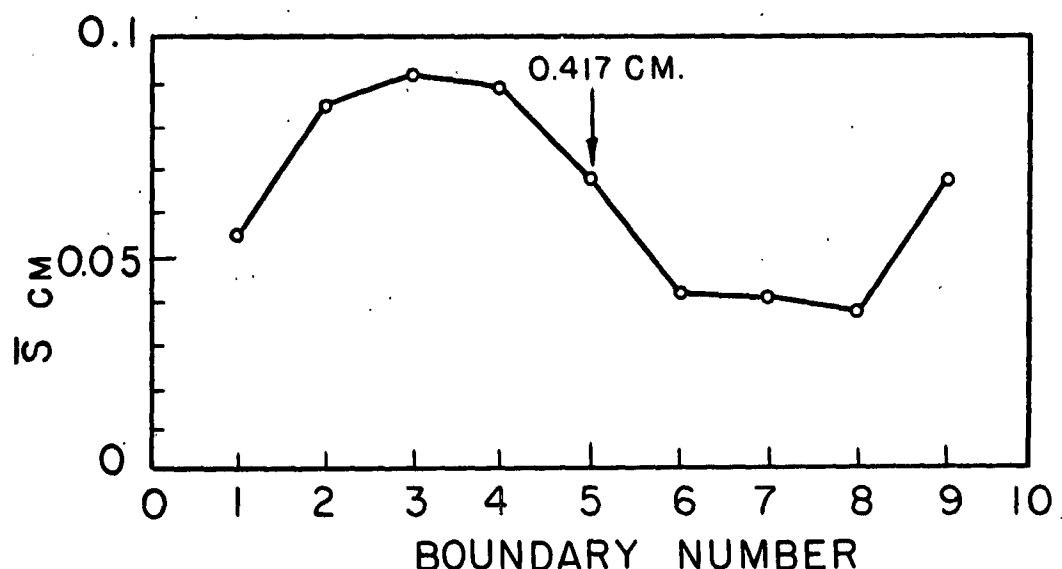


FIG. II BENT CRYSTAL AFTER 168 HOURS AT
412 °C. SPECIMEN 2-B. 9X.



(a)



(b)

FIG.12 AVERAGE INTERBOUNDARY SPACING AS A FUNCTION OF THE ORDER IN WHICH THE BOUNDARIES OCCUR FROM THE SPECIMEN BASE.

(a) SPECIMEN 1-B (b) SPECIMEN 2-B

TABLE V
Results of Bent Crystal Experiment

Spec. No.	θ Max. Deg.	Limit γ Ergs/cm ²	θ Min. Deg.	Limit γ Ergs/cm ²	X Cm.
1-B	0.54	Less than 34	0.31	Less than 19	0.358
2-B	0.62	Greater than 18	0.39	Greater than 11	0.417

Discussion

The results reported here allow, presumably for the first time, an estimate to be made of the absolute energy of a low angle boundary. The essential features previously presented in Tables III and V are shown in Fig. 13 where the energy limits have been plotted as a function of boundary angle. At small angles the Shockley-Read equation

$$E = E_0 \theta \ln \left[\theta_m e / \theta \right]$$

should apply, where for zinc, the theoretical value of E_0 is 1200 ergs/cm² according to the isotropic formula

$$E_0 = \frac{G b}{4(1-\nu)}$$

with the values

$$G = 3.79 \cdot 10^{11} \text{ dyne/cm}^2$$

$$b = 2.66 \cdot 10^{-8} \text{ cm}$$

$$\nu = 0.33$$

A somewhat better value, $E_0 = 1170 \frac{\text{ergs}}{\text{cm}^2}$, is obtained from the anisotropic relations developed by A. J. E. Foreman⁽¹³⁾, using the room temperature

elastic constants taken from Schmid and Boas⁽¹⁸⁾. Elevated temperature elastic constants were not available for zinc. Judging from the behavior of other metals, however, the elastic constants for zinc are probably about 20 percent higher at room temperature than at 412°C. Hence, the value of E_0 at 412°C should be approximately 940 ergs/cm². Assuming this value for E_0 , the energy relation becomes

$$E = 940 \theta \ln \left[\theta_m e / \theta \right]$$

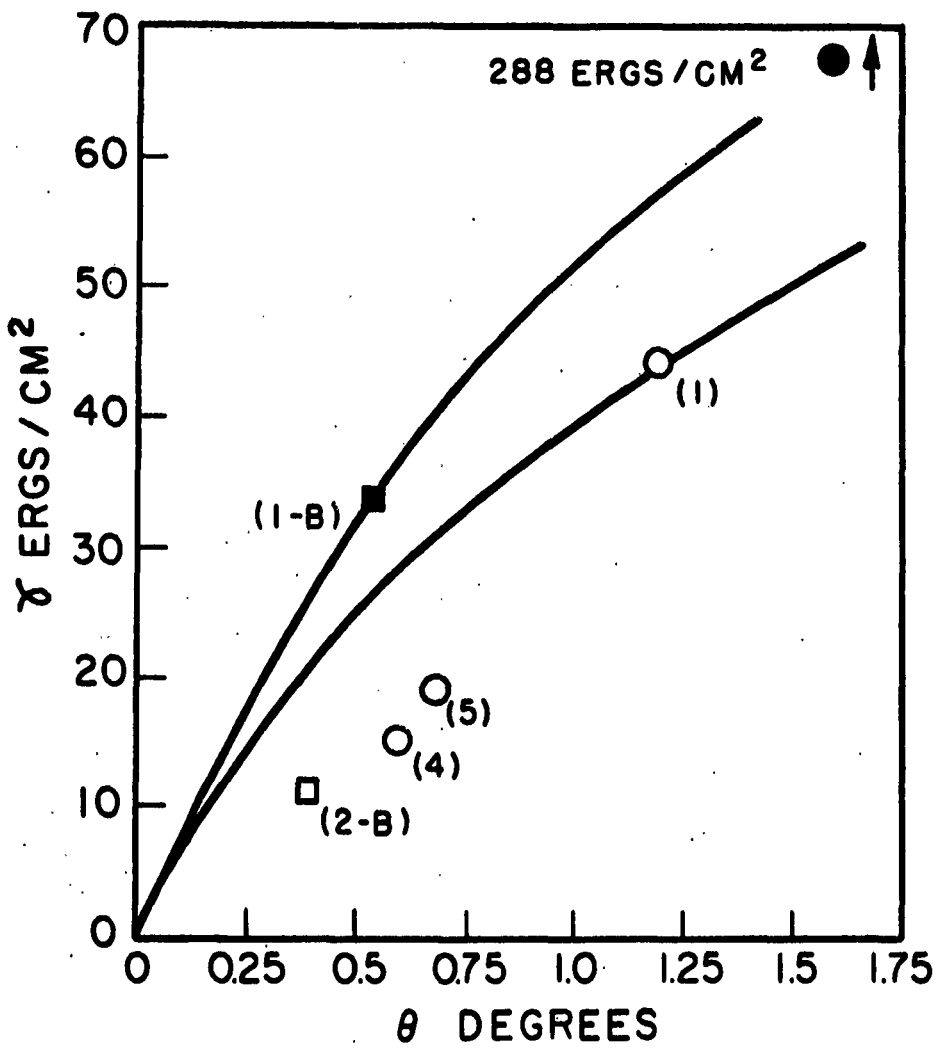
In Fig. 13, curves corresponding to this formula have been drawn through the upper and lower energy limits defined by the experimental data. The two limiting values of θ_m are 9.3 and 4.2 degrees respectively in contrast to those previously reported (page 2) which lie in the range 12 to 30 degrees. This lack of agreement probably arises from a dependence of θ_m on θ . In the present work the results are based upon boundaries of the order of 0.5 degrees, whereas, those derived by Dunn and Lionetti⁽⁶⁾ and others were based on boundaries ranging from 3° to 35° in different materials.

Providing the estimate of E_0 is reasonably correct, the true dependence of energy with angle lies between the two limiting curves. From Fig. 13 the free energy of a one-half degree boundary can be seen to fall in the range

$$\gamma = 29.5 \pm 3.5 \text{ ergs/cm}^2.$$

For a one-half degree boundary there are 3.28×10^5 dislocations per centimeter so that the energy per dislocation for one centimeter of its length is $8.99 \pm 1.07 \times 10^{-5}$ ergs/cm. Since there is one atom per unit cell, this is equivalent to an energy of 1.30 ± 0.15 e.v. per unit cell where the unit cell width is $b \cos 30^\circ$ along the dislocation line.

The strain energy for each dislocation lying in a boundary of angle θ , outside of a small cylinder of radius r_0 round the dislocation (termed the



OPEN POINTS REFER TO LOWER ENERGY LIMITS
 SOLID POINTS REFER TO UPPER ENERGY LIMITS

FIG.13 LOW ANGLE BOUNDARY ENERGY LIMITS PLOTTED
 AGAINST BOUNDARY ANGLE. CURVES ARE DRAWN
 ON THE BASIS OF THE SHOCKLEY-READ FORMULA
 FOR $E_0 = 940$ ERGS/CM².

dislocation core) has been estimated⁽¹⁹⁾ as

$$\mathcal{E} = E_0 b \left[\ln \frac{be}{2\pi r_0} - \ln \theta \right]$$

Taking $r_0 = 3b$, this represents an energy of 1.0 e.v. per unit cell. If the contribution of the entropy is assumed to be approximately - 0.1 e.v., then the energy to be associated with the core for the case quoted above will be of the order 0.4 e.v. per unit cell.

Each of the two methods of energy measurement used in this investigation has certain advantages. The single boundary experiment is theoretically capable of producing accurate results. However, the forces which drive a boundary toward equilibrium diminish progressively as the equilibrium position is approached so that the rate of motion continually decreases. Since a moving boundary encounters obstacles, and because the free energy well is quite shallow, it is not surprising that some boundaries do not move perceptibly in the time available for the experiments. Furthermore, a satisfactory specimen surface condition can only be maintained for a limited time because of the deteriorative effects of high temperature. Therefore, the attainment of equilibrium is practically impossible in this type of experiment.

The bent crystal experiment avoids this difficulty. Since it has many boundaries distributed across the specimen it is only necessary for individual boundaries to move short distances in order to reveal the equilibrium position by virtue of the perturbing effects of "external" forces on the polygonization process. This reduces the time necessary to carry out the experiment. On the other hand, this advantage is gained at the expense of the inherent accuracy of the results. The so-called "normal" region has a certain practical width, and the boundaries within this "normal" region have a range of angles.

One is justified only in extracting the most conservative energy limits from such an experiment.

A knowledge of the approximate energy of a boundary as a function of boundary angle enables one to redesign the experiment for optimum effectiveness. A measure of the sharpness of this energy well is given by the second partial derivative of the total free energy (page 5) with respect to x .

$$\frac{\partial^2 F_T}{\partial x^2} = 2 \delta g t \sin \theta \tan \phi [L - x]$$

As the ratio x/L increases to unity, the more shallow the function $F_T(x)$ becomes. Remembering that x is related to L and θ through equations (1) and (2), it appears that the best compromise lies in choosing the smallest value of x/L that can be accommodated experimentally. An increase in angle ϕ also makes F_T a more sensitive function of x .

REFERENCES

1. J. M. Burgers, "Geometrical Considerations Concerning the Structural Irregularities to be Assumed in a Crystal", Proc. Kon. Ned. Akad. Wet., V. 42, p. 293, (1939) and Proc. Phys. Soc. V. 52, p. 23, (1940).
2. W. L. Bragg, Discussion of a paper by J. M. Burgers, Proc. Phys. Soc., V. 52, p. 54, (1940).
3. R. W. Cahn, "Internal Strains and Recrystallization", Progress in Metal Physics, V. II, Interscience Publishers, N.Y., (1950).
4. A. Guinier and J. Tennevin, "Researches on the Polygonization of Metals", Progress in Metal Physics, V. II, Interscience Publishers, N.Y., (1950).
5. C. S. Smith, Trans. AIME, V. 175, p. 15, (1949).
6. C. G. Dunn and F. Lionetti, Trans. AIME, V. 185, p. 125, (1949).
7. C. G. Dunn, F. W. Daniels, and M. J. Bolton, Trans. AIME, V. 188, p. 368 and p. 1245, (1950).
8. W. Shockley and W. T. Read, Physical Review, V. 75, p. 692; ibid V. 78, p. 275, (1950).
9. W. Shockley and W. T. Read, Imperfections in Nearly Perfect Crystals, John Wiley and Sons Inc., N.Y., Chapter 13, (1950).
10. J. Washburn and E. R. Parker, Trans. AIME, V. 194, p. 1076, (1952).
11. C. H. Li, E. H. Edwards, J. Washburn and E. R. Parker, Acta Metallurgica, V. 1, p. 223, (1953).
12. F. L. Vogel, W. G. Pfann, H. E. Corey, and E. E. Thomas, Phys. Rev., V. 90, p. 489, (1953).
13. A. J. E. Foreman, "Dislocation Energies in Anisotropic Crystals", Acta Metallurgica, V. 3, No. 4, P. 322, (1955).
14. K. T. Aust, B. Chalmers, Proc. Roy. Soc. (London) V. A 201, p. 210; V. A 204, p. 359-366. (1950).
15. A. P. Greenough and R. King, J. Inst. Metals, V. 79, p. 415, (1951).
16. D. W. Bainbridge, C. H. Li, E. H. Edwards, J. Washburn, and E. R. Parker. Univ. of Calif. Inst. of Eng. Research, Fundamental Studies Related to the Origin and Nature of Creep of Metals, Ninth Tech. Report, Series 27, Issue 9, August, 1953.
17. J. Washburn, Univ. of Calif. Inst. of Eng. Research, Fundamental Studies Related to the Origin and Nature of Creep of Metals, Eleventh Tech. Report, Series 27, Issue 11, May, 1954.
18. E. Schmid and W. Boas, Plasticity of Crystals, F. A. Hughes and Co., Ltd., London, (1950).
19. A. H. Cottrell, Dislocation and Plastic Flow in Crystals, 1953, Oxford University Press, p. 95.

TECHNICAL REPORT
Distribution List
N7onr-29516 NR-031-255

	<u>No. of Copies</u>
Chief of Naval Research, Attn: Metallurgy Branch, Code 423, Office of Naval Research, Washington 25, D.C.....	2
Director, Naval Research, Attn: Lab. Technical Information Officer Washington 25, D.C.....	6
Bureau of Aeronautics, USN, Washington D.C.	
N.E. Promisel AE-41.....	3
Tech. Library TD-41.....	1
Bureau of Ordnance, Navy Dept., Washington, D.C.	
ReX.....	3
Tech. Library Ad-3.....	1
Naval Ordnance Lab., Washington, Materials Lab.....	1
U.S. Bureau of Ships, Navy Dept., Washington, D.C.	
Code 330.....	3
Code 337L, Tech. Lib.....	1
U.S. Naval Engineering Exp. Sta., Annapolis, Md., Metals Lab.....	1
N.Y. Naval Shipyard, Director Material Lab., Brooklyn, Code 907.....	1
Post Graduate School, U.S. Naval Academy, Monterey, Calif.,	
Attn: Metallurgy Dept.....	1
Supt., Naval Gun Factory, Washington, D.C.....	1
Director, Naval Research Lab., Washington, D.C.	
Code 700, Metallurgy Division.....	1
Code 186, Tech. Lib.....	1
Chief, Bureau of Yards and Docks, Washington, D.C.....	1
Commanding Officer, U.S. Naval Ordnance Test Station, Inyokern, Calif..	1
Commanding Officer, Naval Air Materiel Center, Philadelphia, Pa.....	1
Commanding Officer, Watertown Arsenal, Massachusetts.....	1
Commanding Officer, Frankford Arsenal, Philadelphia, Pa.....	1
Office of Chief of Engineers, Dept. of Army, Washington, D.C.....	1
U.S. Air Forces Research & Development Division, Washington, D.C.....	1
U.S. Atomic Energy Commission, Division of Research, Washington, D.C...	1
National Bureau of Standards, Washington, D.C.....	1
National Advisory Committee for Aeronautics, Washington, D.C.....	1
Director, Office of Naval Research, Branch Office,	
346 Broadway, New York 13, New York.....	1
Director, Office of Naval Research, Branch Office,	
86 East Randolph St., Chicago 1, Illinois.....	1
Director, Office of Naval Research, Branch Office,	
1000 Geary Street, San Francisco 9, California.....	2
Director, Office of Naval Research, Branch Office,	
1030 East Green Street, Pasadena 1, California.....	1
Dr. Hoylande D. Young, Argonne Nat'l. Lab., P.O. Box 299, Lemont, Ill...	1
B. H. Fry, U. S. Atomic Energy Commission, 1901 Constitution Ave., N.W.	
Washington, D. C.....	2
Carbide and Carbon Chemicals Div., Plant Records Dept.,	
Central Files (K-25), Oak Ridge, Tennessee.....	1
Carbide and Carbon Chemicals Div., Central Reports & Information Office,	
(Y-12), Oak Ridge, Tennessee.....	1

Distribution List (Cont'd.)

	<u>No. of Copies</u>
Miss M. G. Freidank, General Electric Co., Technical Service Div., Tech. Information Group, Richland, Washington.....	1
Dr. F. H. Spedding, Iowa State College, Ames, Iowa.....	1
Document Librarian, Knolls Atomic Power Lab., Schenectady, New York....	1
Document Custodian, Los Alamos Scientific Lab., Los Alamos, New Mexico.	1
Dr. J.J. Burgage, Mound Lab., U.S. Atomic Energy Comm., Miamisburg, Ohio.....	1
Division of Technical Information and Declassification Service, N.Y., Operations Office, Ansonia Station, New York, N.Y.....	1
Central Files, Oak Ridge Nat'l. Lab., Oak Ridge, Tennessee.....	1
Mr. Dale N. Evans, Sandia Corp. Sandia Base, Classified Document Division, Albuquerque, New Mexico.....	1
U.S. Atomic Energy Commission Library Branch, Technical Information, Oak Ridge, Tennessee.....	1
Dr. R. K. Wakerling, Radiation Laboratory, Univ. of California, Berkeley, California.....	1
Librarian, Westinghouse Electric Corp., Atomic Power Div., Pittsburgh, Pa.....	1
Asst. Naval Attache for Research, American Embassy Navy #100, N.Y.....	6
Dr. R. F. Mehl, Carnegie Institute of Technology, Pittsburgh, Pa.....	1
Dr. Robert Maddin, Dept. of Mechanical Engineering, Johns Hopkins Univ.	1
Dr. C. S. Smith, Inst. for Study of Metals, Chicago University.....	1
Dr. Henry Eyring, University of Utah, Salt Lake City, Utah.....	1
Dr. F. A. Biberstein, Jr., Catholic University, Washington, D.C.....	1
Battelle Memorial Institute, Columbus, Ohio, Attn: Mr. H. C. Cross....	1
Mr. A. J. Sindeband, American Electro Metal Corp., Yonkers, N.Y.....	1
Dr. R. L. Fullman, Research Lab., General Electric Co., Schenectady, N.Y.....	1
Prof. Clark, Calif. Institute of Technology, Pasadena, California.....	1
Dr. Finn Jonasson, National Academy of Sciences, Washington, D. C.....	1
Dr. J. S. Koehler, Carnegie Institute of Technology, Pittsburgh, Pa....	1
Prof. M. S. Sack, Cornell University, Ithica, New York.....	1
Prof. W. Prager, Brown University, Providence, Rhode Island.....	1
Dr. L. V. Griffis, Armour Research Foundation, Chicago, Illinois.....	1
Dr. W. C. McGrégor, Univ. of Pennsylvania, Philadelphia, Pa.....	1
Dr. J. E. Dorn, University of California, Berkeley.....	1
University of California, Berkeley, Department of Engineering.....	13
Dr. Frederick Seitz, Physics Dept., University of Illinois, Urbana, Ill	1
Dr. Thorton Read, Bell Telephone Laboratories, Murray Hill Laboratory, Murray Hill, New Jersey.....	1
Prof. P. H. Beck, Dept. of Metallurgy, University of Illinois, Urbana, Ill.....	1
Prof. W. M. Baldwin, Metals Research Lab., Case Inst. of Technology, Cleveland 6, Ohio.....	1
Prof. R. M. Brick, University of Pennsylvania, Philadelphia, Pa.....	1
Prof. Thomas Read, Department of Metallurgy, Columbia Univ., New York, N.Y.....	1
Office of Ordnance Research, Duke University, 2127 Myrtle Drive, Durham, North Carolina, Attn: Dr. A. G. Guy.....	1

Distribution List (Cont'd.)

	<u>No. of Copies</u>
H. Markus, Pitman Dunn Lab. Dept., Frankford Arsenal, Bridge and Tacony Sts., Philadelphia 37, Pa.....	1
Prof. Charles S. Smith, Dept. of Physics, Case Institute of Technology, University Circle, Cleveland 6, Ohio.....	1
Dr. R. D. Potter, 1407 Michelson Lab., China Lake, Inyokern, Calif.....	1
Dr. E. Orowan, Dept. of Mech. Eng., Mass. Inst. of Technology, Cambridge 39, Mass.....	1
Brookhaven National Laboratory, Tech. Information Div., Attn: Research Lib., Upton, Long Island, New York.....	1
Dr. D. S. Billington, Oak Ridge National Laboratory, P.O. Box P, Oak Ridge, Tennessee, Attn: M. L. Bray, Supervisor, Central Files Dept., Information and Reports Division.....	1
John R. Cuthill, Enamelled Metals Section, National Bureau of Standards, Washington 25, D.C.....	1
Dr. N. J. Grant, Department of Metallurgy, Massachusetts Institute of Technology, Cambridge 39, Massachusetts.....	1
Prof. Charles Kittel, Physics Department, University of Calif., Berkeley, Calif.....	1
Prof. M. Cohen, Mass. Institute of Technology, Cambridge 39, Mass.....	1
Prof. A. Goldberg, U.S. Naval Post Graduate School, Monterey, Calif.....	1
Dr. C. S. Barrett, Inst. for the Study of Metals, Chicago University, Chicago, Illinois.....	1
Dr. S. Smoluchowski, Carnegie Inst. of Tech. Schenley Park, Pittsburgh 13, Pa.....	1
Dr. S. Weissmann, Rutgers University, New Brunswick, New Jersey.....	1
Armed Service Technical Information Agency, Document Service Center Knott Building, Dayton 2, Ohio.....	5
Office of Technical Services, Dept. of Commerce, Washington 25, D.C.....	1
E. H. Edwards, 4623 Elmwood Road, Richmond, California.....	1
Dr. George C. Kuczynski, Metallurgy Dept., University of Notre Dame, South Bend, Indiana.....	1
Wright-Air Development Center, Wright-Patterson Air Force Base, Ohio Attn: Materials Lab. (WCRTL-6).....	1
Aeronautical Res. Lab. (WCRR4).....	1
Dr. B. D. Cullity, University of Notre Dame, South Bend, Indiana.....	1
Office of the Commanding Officer, Department of the Army, Pentagon, Washington 25, D. C. Attn: ORDTB, E. L. Hollady.....	2
Dr. B. L. Averbach, Dept. of Metallurgy, Mass. Institute of Technology, Cambridge 39, Massachusetts.....	1
Dr. I. S. Servi, Metals Research Laboratories, P.O. Box 580, Niagara Falls, New York.....	1
Dr. Robert I. Jaffee, Battelle Memorial Inst., 505 King Ave., Columbus 1, Ohio.....	1
Dr. John R. Low, Research Laboratory, General Electric Co., Schenectady, New York.....	1
Dr. E. L. Kamen, Metallurgical Development Sec. K-90, Matls. Engineering Dept., Westinghouse Electric Corp. E. Pittsburgh, Pa.....	1
Carl E. Hartbower, Watertown Arsenal Lab., Watertown 72, Mass.....	1